The lack of antitumor activity of [Pt(DACH)(*N*-R·IDA-*O,N*)] complexes is consistent with a key structure–activity criterion,[3,27] which states that diam(m)ineplatinum(II) complexes must possess a pair of cis (reactive) leaving groups in order to exhibit antitumor activity. Since diam(m)ineplatinum(II) complexes incorporating an O,N-chelating ligand possess only one labile site, the lack of activity of these PtN_3O-type complexes is fully expected and would have been predicted had the structures of the complexes been known prior to biological testing.

The decision to evaluate the antitumor properties of the original homogeneous complexes was made under the presumption that the complexes were pure (based principally on elemental analyses). However, it has been demonstrated indirectly that an active impurity was present in the inactive [Pt(DACH)(*N*-R·IDA)] bulk materials. In retrospect, although these studies were very interesting, the research would not have been initiated were it known that the complexes were impure. This situation (which is perhaps more common in the Pt cancer chemotherapy field than is realized) underscores the need to characterize unequivocally and certify the purity of prospective antitumor complexes before any antitumor testing is initiated, especially when such complexes are derived directly from antitumor-active precursors or starting materials such as [Pt(DACH)SO_4] and [Pt(DACH)Cl_2]. The use of selected spectroscopic techniques and/or reverse-phase HPLC analyses in evaluating the purity of new complexes is highly recommended.

It has been estimated that an impurity level of [Pt(DACH)SO_4] of ≤5% could account for the activity observed for the original crude [Pt(DACH)(*N*-R·IDA)] complexes. We speculate that the active component(s) in the original crude samples tested is most likely derived from [Pt(DACH)SO_4] (as an aquation and/or oligomeric product) or is even perhaps [Pt(DACH)$(OH)_2$].

Acknowledgment. We acknowledge the invaluable assistance of the Microanalysis, Spectroscopy, and Chromatography groups at Parke-Davis and helpful discussions with Dr. L. Marzilli, Emory University.

Registry No. **1**, 61848-66-6; **2**, 62011-40-9; **3**, 66900-68-3; **4**, 61825-94-3; **5**, 82310-65-4; **6** (diastereomer 1), 116558-19-1; **6** (diastereomer 2), 116558-20-4; **7**, 111556-05-9; **8**, 111556-07-1; **9**, 97313-10-5; *N*-Me(IDA), 4408-64-4; *N*-CH_2Ph(IDA), 3987-53-9; [*R,R*-(DACH)D_2-d_6][*d*-tart], 116407-31-9; [*R,R*-(DACH)H_2][*d*-tart], 116407-32-0; [Pt(*R,R*-DACH-d_4)Cl_2], 116407-33-1; [Pt(*R,R*-DACH-d_4)(*N*-Me(IDA))], 116407-34-2; [Pt(*R,S*-DACH)(*N*-Me(IDA))], 116407-35-3; [Pt(*R,S*-DACH)(*N*-CH_2Ph(IDA))], 116407-36-4; D_2, 7782-39-0; ^{195}Pt, 14191-88-9.

(27) (a) Cleare, M. J.; Hoeschele, J. D. *Platinum Met. Rev.* **1973**, *17*, 2. (b) Connors, T. A.; Jones, M.; Ross, W. C. J.; Braddock, P. D.; Kokhar, A. R.; Tobe, M. L. *Chem.-Biol. Interact.* **1972**, *5*, 415; **1975**, *11*, 145.

Contribution from the Biomedical Chemistry Research Center, Department of Chemistry, University of Cincinnati, Cincinnati, Ohio 45221, and Department of Chemistry, Wayne State University, Detroit, Michigan 48202

Thiolato–Technetium Complexes. 1. Synthesis and Characterization of Bis(tertiary diphosphine)technetium(III) Complexes Containing Methanethiolato Ligands. Single-Crystal Structural Analyses of *trans*-[$Tc^{III}(SCH_3)_2(DMPE)_2]CF_3SO_3$ and *trans*-[$Tc^{III}(SCH_3)_2(DEPE)_2]PF_6$, Where DMPE = 1,2-Bis(dimethylphosphino)ethane and DEPE = 1,2-Bis(diethylphosphino)ethane

Takumi Konno,[1,2] Mary Jane Heeg,[3] and Edward Deutsch*,[1]

Received May 24, 1988

The Tc(III) methanethiolato complexes *trans*-$[Tc(SCH_3)_2D_2]^+$, where D is either 1,2-bis(dimethylphosphino)ethane (DMPE) or 1,2-bis(diethylphosphino)ethane (DEPE), have been synthesized and characterized. Preparation of these complexes from $[Tc^V(O)(OH)D_2]^{2+}$ utilizes excess $NaSCH_3$ as reductant and ligand. The X-ray crystal structures of both title complexes are examined. *trans*-$[Tc(SCH_3)_2(DMPE)_2]CF_3SO_3$, chemical formula $TcS_3P_4F_3O_3C_{15}H_{38}$, crystallizes in the triclinic space group $P\bar{1}$ with a = 7.9615 (13) Å, b = 9.3019 (7) Å, c = 18.5029 (16) Å, α = 88.093 (7)°, β = 89.686 (11)°, γ = 88.188 (11)°, V = 1368.8 (3) Å^3, and Z = 2. The final weighted R value is 0.032. The coordination complex is approximately octahedral with average Tc–P = 2.428 Å (range 2.422 (2)–2.434 (2) Å), Tc–S = 2.300 Å (range 2.298 (2)–2.302 (2) Å), and S–C = 1.842 Å (range 1.837 (7)–1.847 (7) Å). *trans*-$[Tc(SCH_3)_2(DEPE)_2]PF_6$, chemical formula $TcS_2P_5F_6C_{22}H_{54}$, crystallizes in the monoclinic space group $P2_1/c$ with a = 11.0724 (13) Å, b = 11.2450 (11) Å, c = 14.1331 (14) Å, β = 107.957 (8)°, V = 1674.0 (3) Å^3, and Z = 2. The final weighted R value is 0.022. This complex is also nearly octahedral with average Tc–P = 2.449 Å (range 2.4399 (8)–2.4584 (7) Å), Tc–S = 2.3025 (5) Å, and S–C = 1.821 (4) Å. In both structures the Tc atom occupies an inversion center. The visible spectra of these *trans*-$[Tc(SCH_3)_2D_2]^+$ complexes in acetonitrile show sulfur-to-technetium charge-transfer bands at 16 810 and 28 490 cm^{-1} for D = DMPE and at 16 610 and 28 830 cm^{-1} for D = DEPE. Cyclic voltammetric measurements in *N,N*-dimethylformamide show two reversible reduction couples corresponding to Tc(III/II) and Tc(II/I) at −0.550 and −1.72 V vs Ag/AgCl for D = DMPE and −0.554 and −1.81 V vs Ag/AgCl for D = DEPE. The absorption spectra and cyclic voltammograms are compared with those of other *trans*-$[TcD_2X_2]^+$ complexes with X = Cl, Br, –NCS and are discussed in terms of the relative strengths of the σ and π interactions between Tc and the ligating S and P atoms.

Introduction

The development of the inorganic chemistry of technetium, including especially the synthesis and characterization of new classes of low-valent complexes, has been driven largely by the preeminence of the isotope ^{99m}Tc in diagnostic nuclear medicine.[4–6] Gratifyingly, applications of the principles and techniques of inorganic chemistry have successfully progressed the aims of nuclear medicine and have generated several new and clinically useful ^{99m}Tc organ imaging agents.[6,7] This laboratory continues to develop new classes of low-valent technetium complexes with the dual goals of elucidating their fundamental inorganic chemistry and evaluating the potential use of their ^{99m}Tc analogues in diagnostic nuclear medicine.

---

(1) University of Cincinnati.

(2) On leave from the Department of Chemistry, The University of Tsukuba, Sakura-Mura, Ibaraki 305, Japan.

(3) Wayne State University.

(4) Deutsch, E.; Libson, K.; Jurisson, S.; Lindoy, L. F. *Prog. Inorg. Chem.* **1983**, *30*, 75–139.

(5) Deutsch, E.; Libson, K. *Comments Inorg. Chem.* **1984**, *3*, 83–103.

(6) Clarke, M. J.; Podbielski, L. *Coord. Chem. Rev.* **1987**, *78*, 253–331.

(7) Deutsch, E.; Gerundini, P.; Fazio, F. In *New Procedure in Nuclear Medicine*; Spencer, R. P., Ed.; CRC: Boca Raton, FL, in press.

0020-1669/88/1327-4113$01.50/0

In this context, a considerable amount of our attention has been focused on the class of complexes *trans*-$[\mathrm{Tc^{III/II}D_2X_2}]^{+/0}$, where D represents a tertiary diphosphine or diarsine chelate and X represents a halide or thiocyanate.[8-13] Complexes in which X = Cl, Br have been well characterized by utilizing macroscopic amounts of ^{99}Tc,[9-11,13,14] and the biological properties of the ^{99m}Tc analogues have been extensively investigated.[8,15-18] *trans*-$[^{99m}\mathrm{Tc^{III}(DMPE)_2Cl_2}]^+$ (where DMPE = 1,2-bis(dimethylphosphino)ethane) was the first cationic ^{99m}Tc complex to be evaluated as a myocardial perfusion imaging agent in humans.[19] Subsequent studies established that this agent fails in humans because it suffers in vivo reduction to the neutral Tc(II) form, *trans*-$[^{99m}\mathrm{Tc^{II}(DMPE)_2Cl_2}]^0$, which washes out of the heart.[20] More recently we have shown in rats that neutral *trans*-$[^{99m}\mathrm{Tc^{II}D_2X_2}]^0$ complexes can cross the blood–brain barrier when D = DMPE or diars (diars = 1,2-bis(dimethylarsino)benzene) and thus might provide the basis for brain perfusion imaging agents.[21]

However, the potential utility of *trans*-$[^{99m}\mathrm{Tc^{III/II}D_2X_2}]^{+/0}$ complexes as organ imaging agents has been limited by the range of X ligands that can be successfully incorporated. Until now, only complexes with X = Cl, Br, –NCS have been readily accessible;[10-12] traversing this series with a constant D ligand leads to only coarse variations in the properties of the resulting *trans*-$[\mathrm{Tc^{III/II}D_2X_2}]^{+/0}$ complexes. In order to construct the detailed structure–activity relationships needed for radiopharmaceutical development, it is necessary to incorporate X ligands that can be systematically varied in relatively small steps. Thiolato ligands, RS$^-$, meet this requirement since a wide variety of subtly differing structures and properties can be incorporated into the organic R group. However, previous attempts to prepare the heterotofore unknown class of *trans*-$[\mathrm{Tc^{III/II}D_2(SR)_2}]^{+/0}$ complexes by substitution of thiolato ligands onto the Tc(III) or Tc(II) halide analogues were unsuccessful, presumably because of the substitution-inert character of these low-valent complexes. In this paper we present an efficient redox synthesis of the prototypical *trans*-$[\mathrm{Tc^{III/II}D_2(SCH_3)_2}]^{+/0}$ complexes, along with their chemical characterization and single-crystal structural analyses of the Tc(III) forms.

Thiolato–technetium complexes are not only of interest because of their potential applications in nuclear medicine. The interactions between nuclear medicine and inorganic chemistry are truly synergistic,[4,5] and these thiolato–technetium complexes will also contribute to our fundamental understanding of several aspects of transition-metal chemistry. For instance, the chemistry of coordinated sulfur is both diverse and intricate, and we have recently reviewed the mechanistic aspects of this chemistry.[22] Well-characterized thiolato complexes of second-row metals are relatively rare, and it is anticipated that investigations of the properties and reactivity profiles of the new class of thiolato complexes presented herein will add significantly to our understanding of the chemistry of coordinated sulfur.

Acronyms and Abbreviations

The following acronyms and abbreviations are used in this article: acac$_2$en = *N,N'*-ethylenebis(acetylacetone iminato); CT = charge transfer; DEPE = 1,2-bis(diethylphosphino)ethane; diars = 1,2-bis(dimethylarsino)benzene; DMF = *N,N*-dimethylformamide; DMPE = 1,2-bis(dimethylphosphino)ethane; DPPE = 1,2-bis(diphenylphosphino)ethane; Et = ethyl; FAB = fast atom bombardment; Me= methyl; PDE = platinum-disk electrode; Ph = phenyl; TEAP = tetraethylammonium perchlorate; TFMS = trifluoromethanesulfonate.

Experimental Section

Caution! Technetium-99 emits a low-energy (0.292-MeV) β particle with a half-life of 2.12×10^5 years. When handled in milligram amounts, ^{99}Tc does not present a serious health hazard since common laboratory materials provide adequate shielding. Bremsstrahlung is not a significant problem due to the low energy of the β-particle emission, but normal radiation safety procedures must be used at all times to prevent contamination. In this paper the symbol Tc refers only to technetium-99; the metastable isotope ^{99m}Tc was not used in these studies.

Reagents. Unless otherwise noted, all chemicals were of reagent grade. Technetium-99 was obtained as ammonium pertechnetate from Oak Ridge National Laboratory and purified as previously described.[10] The DMPE and DEPE ligands were purchased from Strem Chemical Co. and used without further purification. The magic bullet matrix (a 5:1 mixture of dithiothreitol and dithioerythritol in a small amount of methanol) was used in measurements of the FAB mass spectra. DMF labeled "suitable for spectrophotometry" from Burdick and Jackson Laboratories, Inc., and polarographic grade TEAP from G. F. Smith Chemicals were used in the electrochemical measurements.

***trans*-Oxohydroxobis(1,2-bis(dimethylphosphino)ethane)technetium(V) Hexafluorophosphate, *trans*-$[\mathrm{Tc(OH)O(DMPE)_2}](\mathrm{PF_6})_2$.** This synthetic procedure is improved over that previously published.[11] To a solution containing 100 mg of $\mathrm{NH_4TcO_4}$ (5.5×10^{-4} mol) in 4 mL of degassed 0.05 M NaOH was added 420 mg of neat DMPE (2.8×10^{-3} mol), followed by 4 mL of degassed 95% ethanol. After the mixture was stirred at room temperature for 15 min, 0.4 mL of concentrated $\mathrm{CF_3SO_3H}$ was added to the yellow-orange solution. The reaction solution was stirred at room temperature for another 15 min and became deep orange-brown. Adding 2 g of $\mathrm{NH_4PF_6}$ in a small amount of water, followed by cooling in a refrigerator for 1 day, produced an orange precipitate of *trans*-$[\mathrm{Tc(OH)O(DMPE)_2}](\mathrm{PF_6})_2$; yield 350 mg (88%).

***trans*-Bis(methanethiolato)bis(1,2-bis(dimethylphosphino)ethane)technetium(III) Hexafluorophosphate, *trans*-$[\mathrm{Tc(SCH_3)_2(DMPE)_2}]\mathrm{PF_6}$.** To a suspension containing 100 mg of *trans*-$[\mathrm{Tc(OH)O(DMPE)_2}](\mathrm{PF_6})_2$ (1.4×10^{-4} mol) in 20 mL of degassed ethanol was added 100 mg of $\mathrm{NaSCH_3}$ (1.4×10^{-3} mol) in 5 mL of degassed ethanol. The mixture was stirred at 60 °C for 30 min under an argon atmosphere, whereupon the solution became deep purple. To this was added 0.5 mL of saturated $\mathrm{NH_4PF_6}$ in water, and the solution turned blue almost immediately. When the blue solution was cooled to room temperature, a blue precipitate appeared. This blue precipitate was dissolved in a small amount of $\mathrm{CH_3CN}$, and this solution was kept in a refrigerator for 1 day. The resulting crystals of *trans*-$[\mathrm{Tc(SCH_3)_2(DMPE)_2}]\mathrm{PF_6}$ were collected by filtration; yield 30 mg (34%).

***trans*-Bis(methanethiolato)bis(1,2-bis(dimethylphosphino)ethane)technetium(III) Trifluoromethanesulfonate, *trans*-$[\mathrm{Tc(SCH_3)_2(DMPE)_2}]\mathrm{CF_3SO_3}$ (1).** The TFMS salt was obtained by adding $\mathrm{NaCF_3SO_3}$ to an almost saturated solution of *trans*-$[\mathrm{Tc(SCH_3)_2(DMPE)_2}]\mathrm{PF_6}$ in acetone, followed by cooling in a refrigerator for 1 day. Recrystallization from acetone in a refrigerator produced crystals suitable for X-ray analysis.

***trans*-Oxohydroxobis(1,2-bis(diethylphosphino)ethane)technetium(V) Hexafluorophosphate, *trans*-$[\mathrm{Tc(OH)O(DEPE)_2}](\mathrm{PF_6})_2$.** To a solution containing 100 mg of $\mathrm{NH_4TcO_4}$ in 22 mL of degassed 0.1 M NaOH was added 800 mg of neat DEPE (3.88×10^{-3} mol) followed by 4 mL of degassed ethanol. After the yellow solution was stirred at room tem-

---

(8) Deutsch, E.; Bushong, W.; Glavan, K. A.; Elder, R. C.; Sodd, V. J.; Scholz, K. S.; Fortman, D. L.; Lukes, S. J. *Science* (*Washington, D.C.*) **1981**, *214*, 85.

(9) Hurst, R. W.; Heineman, W. R.; Deutsch, E. *Inorg. Chem.* **1981**, *20*, 3298–3303.

(10) Libson, K.; Barnett, B. L.; Deutsch, E. *Inorg. Chem.* **1983**, *22*, 1695–1704.

(11) Vanderheyden, J.-L.; Ketring, A. R.; Libson, K.; Heeg, M. J.; Roecker, L.; Motz, P.; Whittle, R.; Elder, R. C.; Deutsch, E. *Inorg. Chem.* **1984**, *23*, 3184–3191.

(12) Bandoli, G.; Mazzi, U.; Ichimura, A.; Libson, K.; Heineman, W. R.; Deutsch, E. *Inorg. Chem.* **1984**, *23*, 2898–2901.

(13) Ichimura, A.; Heineman, W. R.; Vanderheyden, J.-L.; Deutsch, E. *Inorg. Chem.* **1984**, *23*, 1272–1278.

(14) Elder, R. C.; Whittle, R.; Glavan, K. A.; Johnson, J. F.; Deutsch, E. *Acta Crystallogr., Sect. B* **1980**, *B36*, 1662–1665.

(15) Deutsch, E.; Glavan, K. A.; Sodd, V. J.; Nishiyama, H.; Ferguson, D. L.; Lukes, S. *J. Nucl. Med.* **1981**, *22*, 897–907.

(16) Nishiyama, H.; Adolph, R. J; Deutsch, E.; Sodd, V. J.; Libson, K.; Gerson, M. C.; Saenger, E. L.; Lukes, S. J.; Gabel, M.; Vanderheyden, J.-L.; Fortman, D. L. *J. Nucl. Med.* **1982**, *23*, 1102–1110.

(17) Nishiyama, H.; Deutsch, E.; Adolph, R. J.; Sodd, V. J; Libson, K.; Saenger, E. L.; Gerson, M. C.; Gable, M.; Lukes, S. J.; Vanderheyden, J.-L.; Fortman, D. L.; Scholz, K. S.; Grossman, L. W.; Williams, C. C. *J. Nucl. Med.* **1982**, *23*, 1093–1101.

(18) Vanderheyden, J.-L.; Libson, K.; Nosco, D. L.; Ketring, A. R.; Deutsch, E. *Int. J. Appl. Radiat. Isot.* **1983**, *34*, 1611–1618.

(19) Gerson, M.; Deutsch, E.; Nishiyama, H.; Libson, K.; Adolph, R.; Grossman, L.; Sodd, V.; Fortman, D.; Vanderheyden, J.-L.; Williams, C.; Saenger, E. *Eur. J. Nucl. Med.* **1983**, *8*, 371–374.

(20) Vanderheyden, J.-L.; Heeg, M. J.; Deutsch, E. *Inorg. Chem.* **1985**, *24*, 1666–1673.

(21) Neves, M.; Libson, K.; Deutsch, E. *Nucl. Med. Biol.* **1987**, *14*, 503–510.

(22) Deutsch, E.; Root, M. J.; Nosco, D. L. In *Advances in Inorganic and Bioinorganic Reaction Mechanisms*; Sykes, A. G., Ed.; Academic: London, 1982; Vol. 1, pp 269–389.

perature for 1 h under an argon atmosphere, 0.4 mL of concentrated CF_3SO_3H was added. The reaction solution turned deep orange upon being stirred 30 min longer at room temperature. When 2 g of NH_4PF_6 in a small amount of water was added to the deep orange solution, a white precipitate appeared. After removal of the white precipitate by filtration, the filtrate was kept in a refrigerator for 1 day. Orange crystals of *trans*-$[Tc(OH)O(DEPE)_2](PF_6)_2$ were collected by filtration; yield 300 mg (65%). Anal. Calcd for *trans*-$[Tc(OH)O(DEPE)_2](PF_6)_2$: C, 28.79; H, 5.92; F, 27.32; S, 22.27. Found: C, 28.58; H, 5.57; F, 27.98; S, 21.55.

***trans*-Bis(methanethiolato)bis(1,2-bis(diethylphosphino)ethane)technetium(III) Hexafluorophosphate, *trans*-$[Tc(SCH_3)_2(DEPE)_2]PF_6$ (2).** The *trans*-$[Tc(SCH_3)_2(DEPE)_2]PF_6$ complex was prepared by a method similar to that described above for *trans*-$[Tc(SCH_3)_2(DMPE)_2]PF_6$, using *trans*-$[Tc(OH)O(DEPE)_2](PF_6)_2$ instead of *trans*-$[Tc(OH)O(DMPE)_2](PF_6)_2$. After the blue solution was kept in a refrigerator for 1 day, the resulting crystals of *trans*-$[Tc(SCH_3)_2(DEPE)_2]PF_6$ were collected by filtration; yield 50 mg (48%). The crystals used for X-ray analysis were obtained by slow evaporation from an ethanol solution at room temperature.

Reduction of *trans*-$[Tc(SCH_3)_2D_2]PF_6$, D = DMPE or DEPE. To an anaerobic solution of *trans*-$[Tc(SCH_3)_2D_2]PF_6$ in acetonitrile was added a few drops of $(C_4H_9)_4NBH_4$ in a small amount of ethanol under an argon atmosphere. The blue solution almost immediately turned purple. This purple solution could also be obtined by adding $NaSCH_3$ in a small amount of ethanol to the blue solution. Contact with the air caused the exposed surfaces of the purple solution to turn blue, and bubbling air through the purple solution immediately caused a color change to pale yellow-brown. When several drops of NH_4PF_6 in a small amount of water or an acid such as CF_3SO_3H, HPF_6, or $HClO_4$ was added to the purple solution under an argon atmosphere, the color reverted back to the original blue. No color change occurred when water alone was added to the purple solution. The conversion between blue and purple solutions is reversible for at least four cycles.

Measurements. Elemental analyses were performed by Galbraith Laboratories, Knoxville, TN. Visible-UV spectra were recorded in acetonitrile on a Cary 210 spectrophotometer (Varian) at ambient temperatures. FAB mass spectra were recorded by using the magic bullet matrix on a VG 30-250 spectrometer (VG Instruments, Inc.) at the probe temperature. Xenon was used as the primary beam gas, and the ion gun was operated at 8 keV and 100 μA. Data were collected generally over the mass range 100–1000 Da at 0.7 s/scan. Electrochemical measurements were made with CV-IA apparatus (Bioanalytical Systems, Inc.) using a platinum-disk working electrode (PDE, Bioanalytical Systems, Inc., MF2013). An aqueous Ag/AgCl/NaCl (3 M) electrode and platinum wire were used as reference and auxiliary electrodes, respectively. Electrochemical experiments were conducted in DMF with 0.5 M TEAP as supporting electrolyte and complex concentrations of ca. 10^{-3} M.

Crystallography. Single-crystal X-ray diffraction experiments were performed on a Nicolet R3 automated diffractometer with Mo Kα radiation (λ = 0.7107 Å) and a graphite monochromator at ambient temperature. Details of data collection in common were as follows: scan method $\theta/2\theta$, scan range 1.0° below Kα_1 to 1.0° above Kα_2, scan rate variable 2–5°/min, ratio of background/scan time 0.5. Both structures were solved by Patterson methods and refined in a full matrix with the programs of SHELX-76.[23] All non-hydrogen atoms were refined anisotropically. Neutral atom scattering factors and corrections for anomalous dispersions were from ref 24.

X-ray Characterization of *trans*-$[Tc(SCH_3)_2(DMPE)_2]CF_3SO_3$ (1). Abbreviated crystallographic data are as follows: formula $TcS_3P_4F_3O_3C_{15}H_{38}$, fw 642.46, dark blue rounded cube 0.18 × 0.19 × 0.17 mm³, triclinic crystal system, space group $P\bar{1}$, a = 7.9615 (13) Å, b = 9.3019 (7) Å, c = 18.5029 (16) Å, α = 88.093 (7)°, β = 89.686 (11)°, γ = 88.188 (11)°, V = 1368.8 (3) Å³, Z = 2, F_{000} = 600 e, density (calcd) = 1.559 g cm^{-3}, 2θ range 6–50°, hkl ranges $0 \leq h \leq 10$, $-12 \leq k \leq 12$, $-22 \leq l \leq 23$, 4981 total data collected, 3129 observed data with $I \leq 3\sigma(I)$, μ = 9.98 cm^{-1}, absorption corrections by empirical methods[25] yielded transmission coefficients 0.792–0.738, final conventional R value 0.042, final weighted R value 0.032, weight $(\sigma_F)^{-2}$. Lattice constants were derived from 25 high-angle (2θ > 20°) reflections precisely centered. Four reflections suffered from secondary extinction and were omitted. Hydrogen atoms were placed in observed positions and held invariant. Isotropic temperature factors for the hydrogen atoms were assigned to be equal and refined as a single variable.

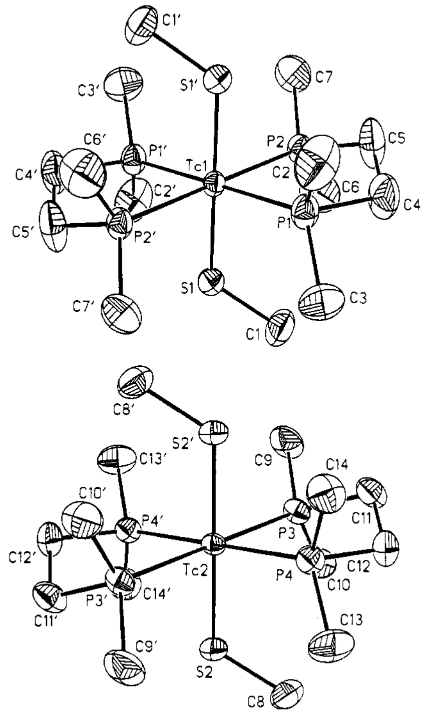

Figure 1. The two independent coordination spheres of Tc in $[Tc(SCH_3)_2(DMPE)_2]^+$. Each Tc atom occupies a crystallographic inversion center. Ellipsoids have been drawn at 50% probability.

X-ray Characterization of *trans*-$[Tc(SCH_3)_2(DEPE)_2]PF_6$ (2). Abbreviated crystallographic data are as follows: formula $TcS_2P_5F_6C_{22}H_{54}$, fw 750.67, dark blue chunk 0.20 × 0.24 × 0.20 mm³, monoclinic crystal system, space group $P2_1/c$, a = 11.0724 (13) Å, b = 11.2450 (11) Å, c = 14.1331 (14) Å, β = 107.957 (8)°, V = 1674.0 (3) Å³, Z = 2, F_{000} = 780 e, density (calcd) = 1.489 g cm^{-3}, 2θ range 6–52°, hkl ranges $0 \leq h \leq 14$, $0 \leq k \leq 14$, $-18 \leq l \leq 18$, discrepancy factor for averaging equivalent reflections R = 0.010, 3688 total data collected, 2611 observed data with $I \geq 2.5\sigma(I)$, μ = 8.2 cm^{-1}, no corrections for absorption or secondary extinction, final R value 0.029, final weighted R value 0.022, weight $(\sigma_F)^{-2}$. Lattice constants were derived from 25 high-angle (2θ > 20°) reflections and constrained to be monoclinic. Hydrogen atoms were placed in observed positions and refined. Some disorder in the PF_6^- group was evident in a final ΔF map.

Results

Synthesis. The methanethiolato–Tc(III) complexes $[Tc(SCH_3)_2D_2]^+$ (D = DMPE, DEPE) can be prepared by reaction of the corresponding Tc^V complexes $[Tc(OH)(O)D_2]^{2+}$ with excess methanethiolate under anaerobic conditions. Addition of a 10-fold excess of $NaSCH_3$ to a suspension of $[Tc(OH)(O)D_2]^{2+}$ in ethanol at 60 °C yields a deep purple solution after 30 min. The purple species is attributed to the Tc(II) complex $[Tc(SCH_3)D_2]^0$ although its isolation from this reaction mixture could not be effected. When an aqueous NH_4PF_6 solution is added to the deep purple solution, the solution quickly changes to a deep blue that is characteristic of the thiolato–Tc(III) product. The oxidation of Tc(II) to Tc(III) also occurs when NH_4^+ is replaced by acids such as CF_3SO_3H and HPF_6. The blue reaction solutions have considerable stability in the air, and the solid Tc(III) complexes $[Tc(SCH_3)_2D_2]PF_6$ can be isolated by slow evaporation and/or cooling of solvent. In contrast, purple solutions of the $[Tc^{II}(SCH_3)_2D_2]$ neutral species tend to decompose, and undergo oxidation to Tc(III), when exposed to air. The isolated blue $[Tc^{III}(SCH_3)_2D_2]^+$ complexes can be reduced to the purple Tc(II) analogues by agents such as CH_3S^- or BH_4^- and can subsequently be regenerated by the addition of acid.

Crystal Structure of *trans*-$[Tc(SCH_3)_2(DMPE)_2]CF_3SO_3$ (1). Figure 1 illustrates the molecular geometry and atomic labeling scheme for the cation. The structure consists of two independent half-cations and a trifluoromethanesulfonate anion. Each Tc atom occupies a crystallographic inversion center. The two independent

---

(23) Sheldrick, G. M. "SHELX-76"; University Chemical Laboratory: Cambridge, England, 1976.

(24) *International Tables for X-ray Crystallography*; Kynoch: Birmingham, England, 1974; Vol. 4 (present distributor D. Reidel, Dordrecht, The Netherlands).

(25) Sheldrick, G. M. "SHELXTL"; University of Göttingen: Göttingen, Federal Republic of Germany, 1978.

Table I. Fractional Atomic Coordinates for $[Tc(SCH_3)_2(DMPE)_2]CF_3SO_3$

atom	*x*	*y*	*z*
Tc1	0.00000	0.00000	0.00000
S1	0.2472 (2)	0.1184 (2)	0.0108 (1)
P1	−0.1490 (3)	0.1443 (2)	0.0877 (1)
P2	−0.1314 (2)	0.1784 (2)	−0.08266 (9)
C1	0.2542 (9)	0.3139 (7)	0.0244 (4)
C2	−0.322 (1)	0.0642 (9)	0.1373 (4)
C3	−0.039 (1)	0.2299 (9)	0.1609 (4)
C4	−0.248 (1)	0.3085 (8)	0.0437 (5)
C5	−0.293 (1)	0.2772 (8)	−0.0335 (4)
C6	−0.006 (1)	0.3203 (9)	−0.1255 (4)
C7	−0.246 (1)	0.1140 (8)	−0.1613 (4)
Tc2	0.00000	0.00000	0.50000
S2	0.2489 (2)	−0.0173 (2)	0.56290 (8)
P3	−0.1328 (2)	0.1790 (2)	0.5763 (1)
P4	−0.1451 (2)	−0.1609 (2)	0.58305 (9)
C8	0.2534 (9)	−0.0406 (7)	0.6619 (4)
C9	−0.2455 (9)	0.3363 (8)	0.5350 (4)
C10	−0.0055 (9)	0.2658 (8)	0.6435 (4)
C11	−0.3016 (8)	0.0951 (7)	0.6291 (4)
C12	−0.2336 (8)	−0.0579 (7)	0.6584 (3)
C13	−0.0375 (9)	−0.3104 (7)	0.6326 (4)
C14	−0.3300 (8)	−0.2505 (7)	0.5492 (4)
S3	0.4514 (3)	0.4637 (2)	0.2374 (1)
O1	0.3070 (6)	0.5324 (6)	0.2664 (3)
O2	0.4861 (7)	0.3208 (5)	0.2617 (4)
O3	0.4809 (8)	0.4913 (7)	0.1619 (3)
C15	0.626 (1)	0.558 (1)	0.2751 (6)
F1	0.6120 (7)	0.6961 (5)	0.2596 (4)
F2	0.7709 (6)	0.5119 (5)	0.2567 (3)
F3	0.6141 (8)	0.5448 (9)	0.3478 (3)

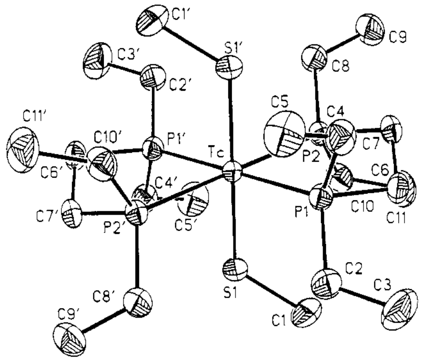

Figure 2. Perspective view of $[Tc(SCH_3)_2(DEPE)_2]^+$. The Tc atom occupies a crystallographic inversion center; ellipsoids represent 50% probability.

coordination spheres are chemically equivalent. All molecular residues are distinct with no unusual intermolecular close contacts. Fractional atomic coordinates are listed in Table I. Bond lengths and angles for the cation are presented in Table II.

Crystal Structure of *trans*-$[Tc(SCH_3)_2(DEPE)_2]PF_6$ (2). Figure 2 illustrates the molecular geometry and atomic labeling scheme for the cation. The structure consists of an independent half-cation and half-anion; the Tc atom and the P atom of the anion both occupy crystallographic inversion centers. No unusual intermolecular close contacts are evident. Fractional atomic coordinates are contained in Table III. Cation bond lengths and angles are given in Table IV. Both complexes **1** and **2** are in trans geometries. The trans configuration is in fact the only geometry that has been observed for $[TcD_2X_2]^{n+}$ complexes, where D represents a bidentate phosphine ligand. The coordination sphere about Tc is approximately octahedral; the most severe deviation from octahedral geometry arises from the usual bite angle of the bidentate phosphine ligand: 81.21 (6) and 81.36 (6)° in **1** and 81.17 (3)° in **2**. Within each cation the two independent P atoms, together with the central Tc atom, define a plane that must necessarily also include the two symmetry-related P atoms. The angle that the Tc–S vector makes with this plane is 83.6 (5) and 83.5 (5)° in **1** and 84.9 (3)° in **2**. A table containing least-squares plane

Table II. Bond Lengths (Å) and Angles (deg) for $[Tc(SCH_3)_2(DMPE)_2]^+$

Tc1–S1	2.298 (2)	Tc2–S2	2.302 (2)
Tc1–P1	2.422 (2)	Tc2–P3	2.431 (2)
Tc1–P2	2.434 (2)	Tc2–P4	2.423 (2)
S1–C1	1.847 (7)	S2–C8	1.837 (7)
P1–C2	1.816 (9)	P3–C9	1.838 (8)
P1–C3	1.834 (8)	P3–C10	1.832 (8)
P1–C4	1.863 (8)	P3–C11	1.836 (7)
P2–C5	1.817 (8)	P4–C12	1.842 (7)
P2–C6	1.836 (9)	P4–C13	1.832 (7)
P2–C7	1.849 (8)	P4–C14	1.838 (7)
C4–C5	1.514 (10)	C11–C12	1.587 (9)
Tc1–S1–C1	122.9 (2)	Tc2–S2–C8	121.7 (2)
Tc1–P1–C2	118.2 (3)	Tc2–P3–C9	120.0 (3)
Tc1–P1–C3	121.8 (3)	Tc2–P3–C10	119.1 (2)
Tc1–P1–C4	111.0 (3)	Tc2–P3–C11	109.1 (2)
Tc1–P2–C5	108.3 (3)	Tc2–P4–C12	109.4 (2)
Tc1–P2–C6	120.3 (3)	Tc2–P4–C13	122.7 (2)
Tc1–P2–C7	118.2 (3)	Tc2–P4–C14	117.6 (2)
S1–Tc1–P1	94.17 (6)	S2–Tc2–P3	95.58 (6)
S1–Tc1–P2	95.47 (6)	S2–Tc2–P4	94.15 (6)
P1–Tc1–P2	81.21 (6)	S3–Tc2–P4	81.36 (6)
P1–C4–C5	109.4 (6)	P3–C11–C12	107.9 (4)
P2–C5–C4	114.7 (6)	P4–C12–C11	109.8 (4)
C2–P1–C3	100.8 (4)	C9–P3–C10	100.7 (3)
C2–P1–C4	103.3 (4)	C9–P3–C11	101.1 (3)
C3–P1–C4	98.7 (4)	C10–P3–C11	104.6 (3)
C5–P2–C6	103.7 (4)	C12–P4–C13	100.8 (3)
C5–P2–C7	103.0 (4)	C12–P4–C14	102.4 (3)
C6–P2–C7	101.2 (4)	C13–P4–C14	101.0 (3)

Table III. Fractional Atomic Coordinates for $[Tc(SCH_3)_2(DEPE)_2]PF_6$

atom	*x*	*y*	*z*
Tc	0.00000	0.00000	0.00000
S1	0.03340 (7)	−0.05157 (7)	0.16375 (5)
P1	0.12238 (7)	0.18336 (7)	0.04370 (6)
P2	0.20676 (7)	−0.07472 (7)	−0.00464 (6)
C1	0.1805 (4)	−0.0130 (5)	0.2596 (3)
C2	0.1097 (4)	0.2735 (3)	0.1486 (3)
C3	0.2181 (4)	0.3592 (5)	0.1942 (4)
C4	0.1093 (3)	0.2975 (3)	−0.0521 (3)
C5	−0.0176 (4)	0.3600 (4)	−0.0897 (4)
C6	0.2925 (3)	0.1479 (3)	0.0736 (3)
C7	0.3102 (3)	0.0546 (3)	0.0011 (3)
C8	0.2124 (3)	−0.1514 (4)	−0.1176 (3)
C9	0.3392 (4)	−0.1611 (4)	−0.1364 (3)
C10	0.2970 (3)	−0.1754 (4)	0.0948 (3)
C11	0.4375 (4)	−0.1579 (5)	0.1426 (4)
P3	0.50000	0.50000	0.00000
F1	0.6331 (2)	0.4425 (2)	0.0081 (2)
F2	0.5701 (3)	0.6137 (3)	0.0505 (3)
F3	0.5091 (3)	0.4476 (3)	0.1034 (2)

Table IV. Bond Lengths (Å) and Angles (deg) for $[Tc(SCH_3)_2(DEPE)_2]^+$

Tc–S1	2.3025 (5)	P2–C8	1.832 (3)
Tc–P1	2.4399 (8)	P2–C10	1.840 (4)
Tc–P2	2.4584 (7)	C2–C3	1.519 (6)
S1–C1	1.821 (4)	C4–C5	1.513 (6)
P1–C2	1.837 (3)	C6–C7	1.521 (4)
P1–C4	1.839 (3)	C8–C9	1.510 (5)
P1–C6	1.843 (3)	C10–C11	1.506 (6)
P2–C7	1.838 (3)		
Tc–S1–C1	121.2 (1)	P1–C4–C5	115.9 (3)
Tc–P1–C2	119.7 (1)	P1–C6–C7	109.3 (2)
Tc–P1–C4	119.5 (1)	P2–C7–C6	111.5 (2)
Tc–P1–C6	108.9 (1)	P2–C8–C9	118.0 (3)
Tc–P2–C7	107.5 (1)	P2–C10–C11	120.3 (3)
Tc–P2–C8	117.8 (1)	C2–P1–C4	101.6 (2)
Tc–P2–C10	118.7 (1)	C2–P1–C6	105.2 (2)
S1–Tc–P1	93.09 (2)	C4–P1–C6	99.4 (2)
S1–Tc–P2	94.50 (2)	C7–P2–C8	102.8 (1)
P1–Tc–P2	81.17 (3)	C7–P2–C10	105.6 (2)
P1–C2–C3	116.4 (3)	C8–P2–C10	102.7 (2)

Table V. Selected Intramolecular Close Contacts (Å) and Torsion Angles (deg) in $[TcD_2(SCH_3)_2]^+$ Complexes (D = DMPE, DEPE)

	$[Tc(SCH_3)_2(DMPE)_2]^+$		
C1–S1–Tc1–P1	−36.8 (3)	C1···C6	3.470 (9)
C1–S1–Tc1–P2	44.8 (3)	C1···C3	3.516 (9)
C8–S2–Tc2–P3	48.5 (3)	C8···C10	3.473 (9)
C8–S2–Tc2–P4	−33.2 (3)	C8···C13	3.525 (9)
	$[Tc(SCH_3)_2(DEPE)_2]^+$		
C1–S1–Tc–P1	−32.9 (2)	C1···C10	3.504 (5)
C1–S1–Tc–P2	48.4 (2)	C1···C2	3.563 (5)

information has been included in the supplementary material. The bidentate phosphine ligand is bound unsymmetrically to the Tc center. Differences in Tc–P length within chelates are 0.012 (3) and 0.008 (3) Å in **1** and 0.019 (1) Å in **2**. Average Tc–P lengths are 2.428 Å in **1** and 2.449 Å in **2**. The unusual P–C distances in the chelate backbone of the cation containing Tc1 of complex **1** are not good estimations of true interatomic distances due to the disorder in the chelate ethylene linkage, which can be seen as large thermal ellipsoids for C4 and C5 in Figure 1. The Tc^{III}–S lengths reported herein are in good agreement as a set: 2.298 (2) and 2.302 (2) Å in **1** and 2.3025 (5) Å in **2**. The orientation of the methanethiolato group with respect to rotation about the Tc–S bond is displaced from a perfectly staggered conformation with respect to the TcP_4 plane. The torsion angles about the Tc–S vector are −36.8 (3) and +44.8 (3)° with respect to P1 and P2, respectively, for the cation containing Tc1 of complex **1**. This results from a close intramolecular contact between the thiol methyl group centered on C1 and the terminal phosphine methyl group centered on C6 bound to P2 (C1···C6 = 3.470 Å). Similar torsional conformations and intramolecular contacts are in evidence for the second cation of **1** and in complex **2**. Table V lists selected torsion angles and intramolecular contacts for these complexes.

As is frequently the case, the anions associated with these structures are less then well-behaved and exhibit high thermal parameters. Average distances and angles for the TFMS anion of **1** are S–O = 1.42 (1) Å, S–C = 1.82 (1) Å, C–F = 1.32 (4) Å, O–S–O = 115.7 (9)°, O–S–C = 102 (2)°, S–C–F = 111 (4)°, and F–C–F = 107 (2)°. The averaged distance and acute angle in the hexafluorophosphate anion of **2** are P–F = 1.56 (2) Å and F–P–F = 89.4 (5)°.

Characterization. In addition to the single-crystal X-ray structural determinations, the methanethiolato complexes are characterized by (i) elemental analyses, (ii) FAB mass spectrometry, and (iii) visible–UV spectrophotometry. The results of these analytical characterizations are summarized in Table VI. The elemental analyses are shown as calculated and determined results and are in acceptable agreement with the proposed formulations. However, compositional assignments are more reliably made by positive-ion FAB mass spectrometry because the small sampling technique of elemental analysis often gives low accuracy and because the interpretation of high-mass positive-ion fragments is not complicated by the presence of coprecipitated simple salts. The positive-ion FAB mass spectrometry spectra show parent peaks at m/z = 493 for $[Tc(SCH_3)_2(DMPE)_2]^+$ and at m/z = 605 for $[Tc(SCH_3)_2(DEPE)_2]^+$, which are consistent with these cations (calculated average masses are 493.5 and 605.7, respectively). Several fragment ions corresponding to losses of CH_3, SCH_3, and/or phosphine groups are also observed and tabulated. A typical FAB-MS spectrum is shown in Figure 3. These complexes also exhibit similar, characteristic, well-defined, intense absorption bands in the visible and UV regions. The visible spectrum of $[Tc(SCH_3)_2(DEPE)_2]^+$ is shown in Figure 4.

Cyclic Voltammetry. The electrochemical studies were performed in 0.5 M TEAP/DMF at a Pt-disk electrode; a summary of these potential measurements is given in Table VI. The methanethiolato–technetium complexes are characterized by two reversible redox couples corresponding to the reactions

$$[Tc^{III}(SCH_3)_2D_2]^+ + e^- \rightarrow [Tc^{II}(SCH_3)_2D_2]^0 \quad (1)$$

$$[Tc^{II}(SCH_3)_2D_2]^0 + e^- \rightarrow [Tc^{I}(SCH_3)_2D_2]^- \quad (2)$$

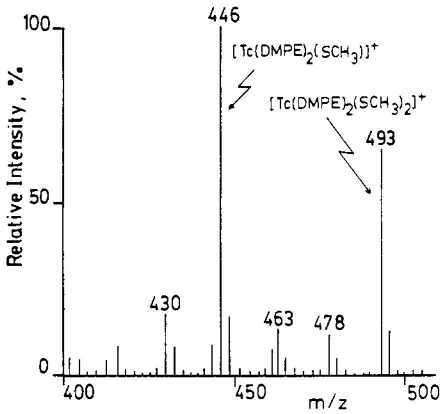

Figure 3. FAB mass spectrum of $[Tc(SCH_3)_2(DMPE)_2](PF_6)$ over the 400–500 m/z range.

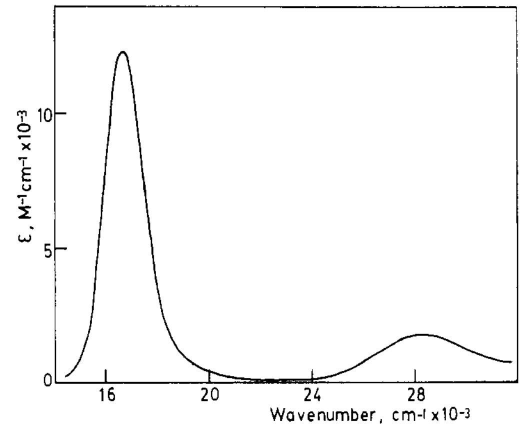

Figure 4. Visible region spectrum of $[Tc(SCH_3)_2(DEPE)_2]^+$ recorded in acetonitrile.

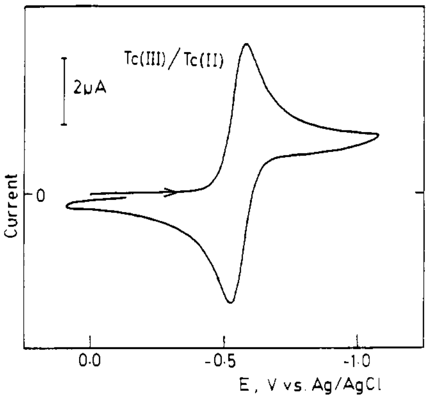

Figure 5. Cyclic voltammogram of 10^{-3} M $[Tc(SCH_3)_2(DEPE)_2]^+$ in 0.5 M TEAP/DMF at a PDE. The scan rate is 100 mV/s.

A typical cyclic voltammogram resulting from reaction 1 is shown in Figure 5. Electrochemical reversibility of this Tc(III/II) couple is established from the observation that (i) the peak current is proportional to the square root of the scan rate, (ii) the ratio of anodic to cathodic peak currents is nearly unity, and (iii) the separation between related cathodic and anodic peaks is close to the Nernstian value of 59 mv for a 1-equiv redox process. The observed peak separations are 60 and 59 mV, for D = DMPE and DEPE, respectively, for reaction 1, which occurs at ∼−0.55 V. The difference in reduction potentials resulting from the differing phosphine substituents of these two complexes is slight for reaction 1: $E^{\circ\prime}$ for $[Tc(SCH_3)_2(DEPE)_2]^+$ is only 4 mV more negative than that for $[Tc(SCH_3)_2(DMPE)_2]^+$. The effect is more profound for reaction 2, where $[Tc(SCH_3)_2(DMPE)_2]^0$ is reduced 90 mV more easily than is the DEPE analogue. An irreversible oxidation is observed (at +925 and +954 mV for D = DMPE and DEPE, respectively) at 25 °C. For $[Tc(SCH_3)_2(DEPE)_2]^+$,

Table VI. Analytical Characterizations of *trans*-$[Tc(SCH_3)_2D_2]^+$ Complexes with D = DMPE, DEPE

Elemental Analyses (%)

		C	H	F	P	S
$[Tc(SCH_3)_2(DMPE)_2]PF_6$	calcd	26.34	6.00	17.86	24.26	10.04
	found	26.36	5.86	16.75	23.40	10.74
$[Tc(SCH_3)_2(DEPE)_2]PF_6$	calcd	35.20	7.25	15.18	20.63	8.54
	found	35.29	7.20	14.89	20.68	8.36

Mass Spectral Data (*m*/*z*)

	complex ion, M^+	fragment ion[f]					
		CH_3	2 CH_3	SCH_3	CH_3, SCH_3	D	D, 2 CH_3
$[Tc(SCH_3)_2(DMPE)_2]^+$	493[a]	478	463	446[a]	430		
$[Tc(SCH_3)_2(DEPE)_2]^+$	605[a]			558		399[a]	369[a]

Visible–UV Spectral Data[b] ($\tilde{\nu}$(max)/10^3 cm^{-1} ($\epsilon/10^3$ M^{-1} cm^{-1}))

$[Tc(SCH_3)_2(DMPE)_2]^+$	16.81 (12.96), 28.49 (1.97), 39.68 (4.85), 46.08 (11.64)
$[Tc(SCH_3)_2(DEPE)_2]^+$	16.61 (12.43), 28.33 (1.81), 38.61 (8.09), 46.08 sh (19.71)

Electrochemical Data[c]

	$E^{\circ\prime}$		
	Tc(III/II)	Tc(II/I)	oxidn, E_{pc}[d]
$[Tc(SCH_3)_2(DMPE)_2]^+$	−0.550	−1.72	+0.925
$[Tc(SCH_3)_2(DEPE)_2]^+$	−0.554	−1.81	+0.954[e]

[a] Intense peak. [b] In acetonitrile; sh denotes a shoulder. [c] At 25 °C in 0.5 M TEAP/DMF at a PDE and with scan rate 100 mV/s. $E^{\circ\prime} = (E_{pc} + E_{pa})/2$ in V vs Ag/AgCl (3 M NaCl) from cyclic voltammetry. [d] Irreversible at 25 °C. [e] Becomes reversible at −70 °C; see text. [f] Fragment ion is M^+ minus the groups shown.

this irreversible oxidation becomes reversible at low temperatures (e.g. −70 °C).

Discussion

Synthesis. While the Tc(III) halide complexes *trans*-$[TcD_2X_2]^+$ (X = Cl, Br) are readily available by a variety of routes,[10,18] they are not useful starting materials for the synthesis of Tc(III) thiolato complexes. Reaction with thiols (or with other reducing ligands such as cyanide, azide, and thiocyanate[10]) does not lead to ligand substitution but yields only reduction of Tc(III) to Tc(II) without modification of the *trans*-$[TcD_2X_2]^{+/0}$ core. In fact, this reduction of Tc(III) halide complexes by thiols provides a convenient preparation of the Tc(II) halide analogues for use in kinetic investigations of electron-transfer reactions.[26]

Synthesis of the methanethiolato Tc(III/II) complexes may be achieved by what has been referred to as a reduction/substitution route.[4] Reaction of excess methanethiol with the Tc(V) complex *trans*-$[TcD_2(O)(OH)]^{2+}$ under anaerobic conditions leads to net reduction of Tc(V) accompanied by substitution of methanethiolate onto the technetium center. This is directly analogous to the synthesis of phosphine-substituted Tc(III) complexes by the reaction of tertiary phosphines with oxo–Tc(V) starting materials.[27] However, while the phosphine reduction/substitution reaction tends to proceed by 2-equiv steps,[18] the thiol reduction/substitution reaction can readily accommodate both 2- and 1-equiv steps. Thus, the initial product generated in the alkaline reaction of *trans*-$[Tc^VD_2(O)(OH)]^{2+}$ with methanethiol is the purple Tc(II) complex:

$$2Tc^VD_2(O)(OH)^{2+} + 8CH_3S^- + 2CH_3SH \rightarrow 2Tc^{II}D_2(SCH_3)_2{}^0 + 3CH_3SSCH_3 + 4OH^- \tag{3}$$

Addition of acid to the reaction medium causes oxidation of the Tc(II) product to the blue Tc(III) complex, presumably by means of the acid-dependent thiol/disulfide redox couple:

$$2Tc^{II}D_2(SCH_3)_2{}^0 + CH_3SSCH_3 + 2H^+ \rightarrow 2Tc^{III}D_2(SCH_3)_2{}^+ + 2CH_3SH \tag{4}$$

The pH-controlled interconversion between Tc(II) and Tc(III) complexes within the reaction mixture appears to be completely reversible; addition of base generates the purple Tc(II) complex, while addition of acid generates the blue Tc(III) complex. Addition of acid to isolated samples of the Tc(II) complex also generates the Tc(III) analogue; the identity of the non-technetium product of this reaction has not been determined, but it may be molecular hydrogen. Stronger reductants, such as borohydride, reduce isolated samples of the Tc(III) complex to the Tc(II) form. However, reaction of the isolated Tc(II) complex with the strong oxidants molecular oxygen and hydrogen peroxide leads to decomposition, suggesting that these agents effect oxidation of the coordinated sulfur atom.[22]

Table VII. Comparison of Spectral and Electrochemical Parameters for $[TcD_2X_2]^+$ Complexes

	LTMCT, $\tilde{\nu}_{max}/cm^{-1}$	$E^{\circ\prime}$(III/II)[a]/ V	$E^{\circ\prime}$(II/I)[a]/ V
$[Tc(DMPE)_2(SCH_3)_2]^+$	16 810, 28 490[b,c]	−0.550[b]	−1.72[b]
$[Tc(DMPE)_2Cl_2]^+$	21 598[d,e]	−0.231[f]	−1.410[f]
$[Tc(DMPE)_2Br_2]^+$	20 121[d,e]	−0.098[f]	−1.268[f]
$[Tc(DEPE)_2(SCH_3)_2]^+$	16 610, 28 830[b,c]	−0.554[b]	−1.81[b]
$[Tc(DEPE)_2Cl_2]^+$	21 552[d,e]	−0.260[f]	−1.439[f,g]
$[Tc(DEPE)_2Br_2]^+$	20 283[d,e]	−0.131[f]	−1.289[f,g]
$[Tc(DPPE)_2(NCS)_2]^+$	17 120[d,h]	+0.390[d]	−0.600[d]
$[Tc(DPPE)_2Cl_2]^+$	21 050[d,e]	−0.001[d]	
$[Tc(DPPE)_2Br_2]^+$	19 840[d,e]	+0.103[d]	

[a] Potentials vs Ag/AgCl (3 M NaCl). [b] This work. [c] In acetonitrile. [d] Reference 10. [e] In ethanol. [f] Reference 13. [g] At −40 °C. [h] In methylene chloride.

Visible–UV Spectra. The *trans*-$[Tc^{III}D_2(SCH_3)_2]^+$ complexes exhibit two characteristic absorption bands in the visible region (Figure 4). The band at lower energy (ca. 17 × 10^3 cm^{-1}) is 6–7 times more intense than that at higher energy (ca. 28 × 10^3 cm^{-1}), but the fact that both bands exhibit extinction coefficients greater than 10^3 M^{-1} cm^{-1} indicates that both arise from charge-transfer (CT) transitions. These CT bands are assigned as arising from sulfur-to-technetium charge-transfer (STTCT) transitions in analogy to the well-documented halogen-to-technetium charge-transfer (HTTCT) bands of *trans*-$[TcX_2D_2]^+$ (X = Cl, Br) complexes.[10,20] This assignment is consistent with the following observations:

(1) The lowest energy STTCT (ca. 17 × 10^3 cm^{-1}) occurs at much lower energy than do the HTTCT's in analogous chloro (ca.

---

(26) Libson, K.; Doyle, M. N.; Thomas, R. W.; Nelesnik, T.; Woods, M.; Sullivan, J. C.; Elder, R. C.; Deutsch, E. *Inorg. Chem.* **1988**, *27*, 3614–3619.

(27) Jurisson, S. S.; Dancey, K.; McPartlin, M.; Tasker, P. A.; Deutsch, E. *Inorg. Chem.* **1984**, *23*, 4743–4749.

21.5×10^3 cm^{-1}) and bromo (ca. 20×10^3 cm^{-1}) complexes (Table VII). This is to be expected since methanethiolate is a much better reducing agent than either bromide or chloride. Thus, the ordering of lowest energy CT bands ($E([TcD_2Cl_2]^+) > E([TcD_2Br_2]^+) > E([TcD_2(SCH_3)_2]^+)$) is opposite to the order of reducing power of the axial ligands ($^-SCH_3 > Br^- > Cl^-$).

(2) Reduction of Tc(III) to Tc(II) causes a blue shift of the lowest energy STTCT from ca. 17×10^3 cm^{-1} to ca. 19×10^3 cm^{-1}, reflecting the fact that Tc(II) is a poorer oxidant than is Tc(III).

Coordinated halogens or thiols should give rise to two classes of LTMCT (ligand-to-metal CT) bands, one each arising from the π and σ orbitals of the coordinated atoms. Two HTMCT bands are observed in *trans*-$[Re^{III}D_2Cl_2]^+$ complexes,[20] and two STTCT bands are observed for each of the *trans*-$[Tc^{III}D_2(SCH_3)_2]^+$ complexes studied here. However, only one HTTCT band is observed in *trans*-$[Tc^{III}D_2X_2]^+$ complexes.[10,13] Considering that the two HTMCT bands in the analogous Re(III) complex are only separated by 1.2×10^3 cm^{-1},[20] it is likely that this single HTTCT band in Tc(III) complexes represents two unresolved CT transitions that presumably originate from the π and σ halogen orbitals. In marked contrast, the two STTCT transitions of *trans*-$[Tc^{III}D_2(SCH_3)_2]^+$ are separated by ca. 12×10^3 cm^{-1}, indicating that in these complexes the sulfur-based orbitals from which these transitions originate have considerably different energies. Arguments presented below support the assignment of the lower energy STTCT transition as S(π) to Tc, while that at higher energy may be assigned to S(σ) to Tc. These assignments are consistent with the expected differences in the chemistries of coordinated sulfur and coordinated halides and with the fact that the CT terminates on a t_{2g} orbital of π symmetry.

The *trans*-$[Tc^{III}D_2(SCH_3)_2]^+$ complexes (D = DMPE, DEPE) also exhibit intense bands in the UV region (at ca. 39×10^3 cm^{-1}). The energies of these bands are more sensitive to the nature of the D ligand than are the energies of the STTCT bands in the visible region, and on this basis they are assigned as arising from phosphorus-to-technetium CT transitions. Analogous phosphorus-to-technetium CT transitions are observed in the DMPE and DEPE complexes *trans*-$[MD_2Cl_2]^{+/0}$ (M = Tc, Re)[13,20] and $[TcD_3]^+$.[13]

Cyclic Voltammetry. The data of Table VII show that the *trans*-$[Tc^{III}D_2(SCH_3)_2]^+$ complexes are much more difficult to reduce from Tc(III) to Tc(II) than are the corresponding halide complexes *trans*-$[Tc^{III}D_2X_2]^+$ (X = Cl, Br). The difference in reduction potentials is about 300 mV for the chloro complex and about 400 mV for the bromo complex. The same effect is observed for reduction of Tc(II) to Tc(I), and the potential differences are even larger. Thus, for both the Tc(III/II) and Tc(II/I) couples, replacement of halide ligands by methanethiolates in the *trans*-$[TcD_2X_2]^{+/0/-}$ core dramatically stabilizes the higher oxidation state. This large effect arises primarily from the strong electron-donating character of thiolato ligands,[28] which stabilizes higher oxidation states by donation of σ-electron density.

Among the four X ligands described in Table VII ($-NCS^-$, Cl^-, Br^-, and $^-SCH_3$), the strong σ-donating character of the Brønsted base methanethiolate adequately explains its unique stabilization of higher technetium oxidation states. Since the other three ligands are very weak Brønsted bases and are thus uniformly poor σ donors, their relative effects on redox potentials presumably arise primarily from π-bonding interactions. Reduction potentials in Tc(III)/Tc(II)/Tc(I) complexes reflect relative energies of the t_{2g} nonbonding metal orbitals, and it is precisely these orbitals that have the proper symmetry to interact with ligand-centered π orbitals. Previous studies on ruthenium(III/II) complexes have shown that metal–ligand π interactions are reflected in redox potentials and that $-NCS$ can function as a weak π-acceptor ligand.[29,30] In this context the ordering of Tc(III/II) redox potentials $E°'(X = -NCS) > E°'(X = Br) > E°'(X = Cl) > E°'(X = SCH_3)$ is seen to result from combined σ- and π-bonding effects, with the first three members of the series being ranked by their relative tendency to accept π-eletron density from the technetium center.

The data of Table VII show that reduction potentials for Tc(III/II) and Tc(II/I) couples also depend somewhat on the nature of the D ligand.[10,13] The ordering of potentials $E°'(D = DEPE) < E°'(D = DMPE) < E°'(D = DPPE)$ observed for these technetium couples is also observed for analogous Re(III/II) and Re(II/I) couples.[31] In general, DEPE complexes are more difficult to reduce than the DMPE analogues, presumably because DEPE is a better σ donor that provides greater stabilization of the higher oxidation states. (1) For M(III/II) couples this effect averages about 31 mV for the *trans*-$[TcD_2X_2]^{+/0}$ (X = Cl, Br) complexes and about 27 mV for the analogous Re complexes. However, this effect is greatly reduced when X is the strongly σ-donating methanethiolate ligand, possibly due to saturation of the σ-accepting ability of the Tc(III) center. (2) For M(II/I) couples this effect averages about 25 mV for the *trans*-$[TcD_2X_2]^{0/-}$ (X = Cl, Br) complexes, is 50 mV for *trans*-$[ReD_2Cl_2]^{0/-}$, and is 146 mV for $[TcD_3]^{2+/+}$. When X = $^-SCH_3$, this effect of varying D on the *trans*-$[TcD_2(SCH_3)_2]^{0/-}$ couple is about 100 mV. Further studies will be required to fully understand the dependence of redox potentials on D and X identity as a function of metal oxidation state.

Each of the *trans*-$[Tc^{III}D_2(SCH_3)_2]^+$ complexes exhibits an irreversible oxidation wave at room temperature, which becomes reversible at low temperatures for the complex with D = DEPE. Since electrochemical oxidations of sulfur-containing species are generally irreversible,[22] this latter observation implies that the redox process which gives rise to this oxidation wave involves the technetium center rather than the coordinated sulfur atom.

Relationships between $E°'$ and LTMCT Energy. The potential at which a central metal undergoes reduction is an inherent component of the energy of any ligand-to-metal charge-transfer transition (E_{LTMCT}). For a series of closely related complexes, a linear correlation betweeen reduction potential and E_{LTMCT} can be anticipated—the easier a complex is to reduce, the lower will be E_{LTMCT}. Such linear correlations have been observed for *trans*-$[MD_2X_2]^{+/0}$ (M = Tc, Re; X = Cl, Br, –NSC) complexes.[10,31] For these three ligands there is no ambiguity in constructing such correlations since only one LTMCT band is observed; this single band presumably represents the unresolved transitions from ligand orbitals of σ and π symmetry (vide supra). However, for X = $^-SCH_3$, the observation of two LTMCT bands complicates the situation.

For *trans*-$[TcD_2X_2]^+$ complexes, when X = Cl the Tc(III) center is harder to reduce than when X = Br and, correspondingly, the HTTCT band occurs at higher energies for Cl than for Br (Table VII). When X = SCH_3, the strong σ-donating properties of this ligand make Tc(III) much harder to reduce than when X = Cl and thus the *corresponding* CT band should occur at even higher energy than observed for the Cl or Br complexes. Within this analysis, the higher energy STTCT band (at ca. 28×10^3 cm^{-1}) of the *trans*-$[Tc^{III}D_2(SCH_3)_2]^+$ complexes thus presumably corresponds to the S(σ)-to-technetium CT transition. The lower energy STTCT band (at ca. 17×10^3 cm^{-1}) therefore corresponds to the S(π)-to-technetium CT transition. The very low energy of this S(π)-to-technetium CT is presumably derived from the inherent reducing power of the thiolato ligand—it is the nonbonded (π) electron pairs of the coordinated sulfur atom that are available for reduction since the bonding (σ) electron pair is stabilized by interaction with the technetium center.

From this analysis it is seen that the occurrence of remarkably low-energy LTMCT bands for *trans*-$[Tc(DPPE)_2(NCS)_2]^+$ and the two *trans*-$[TcD_2(SCH_3)_2]^+$ (D = DMPE, DEPE) complexes (Table VII) arise from different causes. For the –NCS complex the LTMCT is composed of unresolved σ and π transitions, and

---

(28) Blower, P. J.; Dilworth, J. R. *Coord. Chem. Rev.* **1987**, *76*, 121–185.
(29) Lim, H. S.; Barclay, D. J.; Anson, F. C. *Inorg. Chem.* **1972**, *11*, 1460–1466.
(30) Zwickel, A. M; Creutz, C. *Inorg. Chem.* **1971**, *10*, 2395–3113.
(31) Kirchhoff, J. R.; Heineman, W. R.; Deutsch, E. *Inorg. Chem.* **1987**, *26*, 3108–3113.

Table VIII. Technetium–Phosphorus Bond Lengths (Å) in Six-Coordinate Complexes[a,b]

	Tc–P	ref
	Tc^{I}	
$[Tc(DPPE)_2(N_2)(H)]$	2.373, 2.363, 2.340, 2.358	40
$[Tc(PMe_2Ph)_2(CO)_2(dpa)]$	2.431, 2.387	41
$[Tc(PMe_2Ph)_2(CO)_2(dtt)]$	2.422, 2.390	41
$[Tc(PPh(OEt)_2)_4(CO)_2]^+$	2.414, 2.379	42
av, range for Tc^{I}	2.39 (3), 2.34–2.43	
	Tc^{II}	
$[Tc(PPh(OEt)_2)_4Cl_2]$	2.408, 2.425, 2.408, 2.405	43
$[Tc(DPPE)_2(NCS)_2]$	2.436, 2.441, 2.421, 2.450	12
$[Tc(DPPE)_2Cl_2]$	2.444, 2.417, 2.444, 2.410	26
av, range for Tc^{II}	2.43 (2), 2.41–2.45	
	Tc^{III}	
$[Tc(DMPE)_2Cl_2]^+$	2.432, 2.433, 2.443, 2.437	11
$[Tc(DPPE)_2Br_2]^+$	2.487, 2.513	10
$[Tc(DPPE)_2Cl_2]^+$	2.509, 2.492	26
$[Tc(PMe_2Ph)_3Cl_3]$	2.468, 2.478, 2.463, 2.480	44
$[Tc(PPh_3)_2(acac_2en)]^+$	2.499, 2.511, 2.524, 2.497	27
$[Tc(DMPE)_2(SCH_3)_2]^+$	2.434, 2.422, 2.431, 2.423	this work
$[Tc(DEPE)_2(SCH_3)_2]^+$	2.458, 2.440	this work
av, range for Tc^{III}	2.46 (3), 2.42–2.52	
	Tc^{V}	
$[Tc(PPh_3)_2(N)(NCS)_2(CH_3CN)]$	2.494, 2.525	45
$[Tc(O)(OH)(DMPE)_2]^{2+}$	2.473, 2.480	11
av, range for Tc^{V}	2.49 (2), 2.47–2.53	

[a] Tc–P distances are tabulated only for complexes in which the trans ligand is also a phosphine (i.e., P–Tc–P is in the range 160–180°). [b] Abbreviations are as follows: DPPE = 1,2-bis(diphenylphosphino)ethane, Me = methyl, Ph = phenyl, Et = Ethyl, dpa = *N,N'*-diphenylacetamidinato, dtt = *N,N'*-ditolyltriazenido, DMPE = 1,2-bis(dimethylphosphino)ethane, acac₂en = *N,N'*-ethylenebis(acetylacetone iminato).

the low value of E_{LTMCT} results from stabilization of the Tc(II) center by the π-accepting –NCS and DPPE ligands. For the two methanethiolato complexes, the low-energy STMCT band represents a S(π)-to-technetium CT; the low value of E_{LTMCT} results not from stabilization of the Tc(II) center but rather from the inherent reducing power of the nonbonding electrons on the coordinated thiolato ligand.

Crystallography. The technetium complexes reported herein are remarkably similar. They exhibit analogous distortions from perfect octahedral geometry that are induced by the bite angle of the bis(dialkylphosphino)ethane chelate. The acute bite angle distorts the rectangular base defined by the two coplanar bidentate phosphine ligands to a planar rhomboid base. The axial unidentate thiolato ligands are then skewed toward the more acute point in the rhomboidal base, i.e. the basal ligand furthest from the central metal ion. Hence, the inequivalence of the Tc–P distances and the nonorthogonal Tc–S vector with respect to the TcP_4 plane are due to steric factors. This distortion of trans-octahedral geometry into a skew-rhomboid geometry is an alternative to the skew-trapezoidal distortion discussed by Kepert.[32] When the molecules occupy an inversion center as do those reported here, the skew-trapezoidal distortion is disallowed and only the observed skew-rhomboid distortion is permitted. An interesting aside is that the onset of these distortions from octahedral geometry is observed at larger "normalized bite" values, b (in Kepert's nomenclature $b = 2 \sin ((\text{bite angle})/2)$), than previously ascertained by Kepert. He has predicted undistorted trans-octahedral geometries for $b \approx 1.2$–1.5. For reference, orthogonal bite angles have $b = 1.414$ and the phosphine ligands in this work have $b = 1.30$.

Previously published reports of structures containing Tc–P bonds that are trans to other phosphine ligands include 14 complexes and 42 Tc–P observations. These data, along with data from the present work, are collected in Table VIII, sorted by Tc oxidation state. The average Tc–P length for oxidation states I, II, III, and V show a well-substantiated trend of decreasing bond distance with decreasing oxidation state, even though such obvious influences as overall charge, identity of the other ligands in the complex, and differing substituents on phosphorus are not considered. Only when M→L back-bonding is an important mode of bonding does the metal–ligand interaction increase with increasing electron density at the metal center.

The average Tc–P distances in the present work, 2.43 (1) Å for **1** and 2.45 (1) Å for **2**, are in good agreement with that reported[11] for *trans*-$[Tc(DMPE)_2Cl_2]^+$; i.e., changing the axial ligands from Cl^- to $^-SCH_3$ has little effect on the equatorial Tc–P distances. If the Tc(III) entries of Table VIII are grouped according to the substituents on P, it is seen that (i) $[Tc(DMPE)_2(SCH_3)_2]^+$ and $[Tc(DMPE)_2Cl_2]^+$ have predominantly methyl substituents on P and their Tc–P distances average 2.43 and 2.44 Å, respectively, (ii) $[Tc(DEPE)_2(SCH_3)_2]^+$ has predominantly ethyl substituents on P and Tc–P averages 2.45 Å, (iii) the complexes $[Tc(DPPE)Br_2]^+$, $[Tc(DPPE)_2Cl_2]^+$, and $[Tc(PPh_3)_2(acac_2en)]^+$ contain predominantly phenyl substituents and their Tc–P distances average 2.50, 2.50, and 2.51 Å, respectively, and (iv) the remaining Tc^{III} complex, $[Tc(PMe_2Ph)_3Cl_3]$, has mixed substituents on P and possesses a Tc–P average distance of 2.47 Å, which is midway between the methyl- and phenylphosphine values. On this basis it appears that on average Tc^{III}–P lengths increase as the group bonded to P varies as Me < Et < Ph, although the magnitude of change is small. This ordering can result entirely from steric factors, and thus there is no reason to invoke electronic origins.

The averaged Tc–S distances in **1** and **2** (2.300 (3) and 2.3025 (5) Å, respectively) are in good agreement with technetium–thiolato lengths in $[Tc^{V}O(SCH_2CH_2S)]^-$ (2.30 (1) Å),[33] $[Tc^{V}O(SC_5H_9NO_2)(SC_5H_{10}NO_2)]$ (2.29 (1) Å),[34] $[Tc^{V}O(SCH_2COS)_2]^-$ (2.32 (2) Å),[35] $[Tc^{V}O(SCH_2CH_2O)_2]^-$ (2.29 (1) Å),[36] and $[Tc^{V}O(S_2O_4C_6H_8)_2]^-$ (2.31 (1) Å)[37] and also with the rhenium–thiolato distance in $[Re^{V}S(SCH_2CH_2S)_2]^-$ (2.30 (1) Å).[38] Although the just-mentioned comparison complexes contain Tc and Re in a +5 oxidation state, they also all contain strong multiply bound π-donor ligands that increase the effective metal electron density. Other common technetium–sulfur compounds are those in which the sulfur atom is part of a dithiocarbamato ligand, and these typically exhibit somewhat longer Tc–S lengths (2.40–2.50 Å).[39]

Acknowledgment. Financial support was provided in part by National Institutes of Health Grants HL-21276 and CA-42179 and by Mallinckrodt, Inc. The diffractometer used herein was

---

(32) Kepert, D. L. *Inorganic Stereochemistry*; Springer-Verlag: New York, 1982; p 86 ff.

(33) Smith, J. E.; Byrne, E. F.; Cotton, F. A.; Sekutowski, J. C. *J. Am. Chem. Soc.* **1978**, *100*, 5571–5572.

(34) Franklin, K. J.; Howard-Lock, H. E.; Lock, C. J. L. *Inorg. Chem.* **1982**, *21*, 1941–1946.

(35) DePamphilis, B. V.; Jones, A. G.; Davis, M. A.; Davison, A. *J. Am. Chem. Soc.* **1978**, *100*, 5570–5571.

(36) Jones, A. G.; DePamphilis, B. V.; Davison, A. *Inorg. Chem.* **1981**, *20*, 1617–1618.

(37) Bandoli, G.; Nicolini, M.; Mazzi, U.; Spies, H.; Munze, R. *Transition Met. Chem.* (*London*) **1984**, *9*, 127–129.

(38) Blower, P. J.; Dilworth, J. R.; Hutchinson, J. P.; Zubieta, J. A. *Inorg. Chim. Acta* **1982**, *65*, L225–226.

(39) Baldas, J.; Bonnyman, J. B.; Pojer, P. M.; Williams, G. A.; Mackay, M. F. *J. Chem. Soc., Dalton Trans.* **1981**, 1798–1801; **1982**, 451–455. Batsanov, A. S.; Struchkov, Y. T.; Lorenz, B.; Wahren, M. *Z. Anorg. Allg. Chem.* **1984**, *510*, 117–122. Baldas, J.; Bonnyman, J.; Mackay, M. F.; Williams, G. A. *Aust. J. Chem.* **184**, *37*, 751–759.

(40) Struchkov, Y. T.; Bazanov, A. S.; Kaden, L.; Lorenz, B.; Wahren, M.; Meyer, H. *Z. Anorg. Allg. Chem.* **1982**, *494*, 91–97.

(41) Marchi, A.; Rossi, R.; Duatti, A.; Magon, L.; Bertolasi, V.; Ferretti, V.; Gilli, G. *Inorg. Chem.* **1985**, *24*, 4744–4748.

(42) Cingi, M. B.; Clemente, D. A.; Magon, L.; Mazzi, U. *Inorg. Chim. Acta* **1975**, *13*, 47–59.

(43) Mazzi, U.; Clemente, D. A.; Bandoli, G.; Magon, L.; Orio, A. A. *Inorg. Chem.* **1977**, *16*, 1042–1048.

(44) Bandoli, G.; Clemente, D. A.; Mazzi, U. *J. Chem. Soc., Dalton Trans.* **1976**, 125–130.

(45) Baldas, J.; Bonnyman, J.; Williams, G. A. *J. Chem. Soc., Dalton Trans.* **1984**, 833–837.

Inorg. Chem. **1988**, *27*, 4121–4127

purchased through an NSF equipment grant to Wayne State University. M.J.H. continues to appreciate the expertise of L. Boulet and the WSU Electornics Shop.

Registry No. **1**, 116840-44-9; **2**, 116840-46-1; *trans*-$[Tc(OH)O(DMPE)_2](PF_6)_2$, 116840-47-2; NH_4TcO_4, 34035-97-7; *trans*-$[Tc(SCH_3)_2(DMPE)_2]PF_6$, 116862-78-3; *trans*-$[Tc(OH)O(DEPE)_2](PF_6)_2$, 116862-80-7; $Tc(SCH_3)_2(DMPE)_2$, 116840-48-3; $Tc(SCH_3)_2(DEPE)_2$, 116840-49-4; $[Tc(SCH_3)_2(DMPE)_2]^-$, 116840-50-7; $[Tc(SCH_3)_2(DEPE)_2]^-$, 116840-51-8.

Supplementary Material Available: Tables A–E, listing thermal parameters for **1**, hydrogen parameters for **1**, thermal parameters for **2**, hydrogen parameters for **2**, and least-squares planes (5 pages); tables of calculated and observed structure factors for **1** and for **2** (54 pages). Ordering information is given on any current masthead page.

Contribution from the Instituto di Chimica e Tecnologia dei Radioelementi del CNR, Area della Ricerca,
Corso Stati Uniti 4, 35100 Padova, Italy, Biomedical Chemistry Research Center, Department of Chemistry, University of Cincinnati,
Cincinnati, Ohio 45221-0172, and Dipartimento di Chimica, Universitá di Sassari, Via Vienna 2, 07100 Sassari, Italy

Electrochemistry of Oxo–Technetium(V) Complexes Containing Schiff Base and 8-Quinolinol Ligands

Fiorenzo Refosco,[1] Ulderico Mazzi,[1] Edward Deutsch,*[2] Jon R. Kirchhoff,[2] William R. Heineman,[2] and Renato Seeber[3]

Received April 19, 1988

The electrochemistry of six-coordinate, monooxo technetium(V) complexes containing Schiff base ligands has been studied in acetonitrile and *N,N'*-dimethylformamide solutions. The complexes have the general formula $TcOCl(L_B)_2$ or $TcO(L_T)(L_B)$, where L_B represents a bidentate-N,O Schiff base ligand or a bidentate-N,O 8-quinolinol ligand and L_T represents a tridentate-O,N,O Schiff base ligand. Cyclic voltammetry at a platinum-disk electrode, controlled-potential coulometry, and thin-layer spectroelectrochemistry were used to probe both the oxidation and the reduction of these complexes. The results of these studies, and previously reported results on the analogous Re(V) complexes, can be understood within a single general reaction scheme. The salient features of this scheme are (i) one-electron reduction of Tc(V) to Tc(IV), (ii) subsequent loss of a ligand situated cis to the $Tc{=}O$ linkage, and (iii) subsequent isomerization of this unstable Tc(IV) product to a more stable complex in which the site trans to the $Tc{=}O$ linkage is vacant. The Tc(IV) complexes can also be reduced to analogous Tc(III) species, which appear to undergo the same ligand loss and isomerization reactions. The technetium complexes are 400–500 mV easier to reduce than are their rhenium analogues. The 8-quinolinol ligands, and especially the 5-nitro derivative, both thermodynamically and kinetically stabilize the Tc(IV) and Tc(III) oxidation states. These electrogenerated species are unusual in that they constitute the bulk of the known examples of monomeric Tc(IV) and Tc(III) complexes containing only N- and O-donating ligands.

Introduction

In the past several years considerable effort[4–14] has been focused on the electrochemistry of technetium complexes containing this element in oxidation states ranging from +1 to +3. This focus stems partly from the importance of low-valent technetium-99 complexes, and their associated in vivo redox chemistry, in nuclear medicine.[15–19] These electrochemical studies have been facilitated by the fact that the π-acid ligands used to stabilize low oxidation states of technetium also tend to promote facile, electrochemically reversible, electron-transfer reactions.[20,21]

Technetium(V) complexes containing the monooxo TcO^{3+} or dioxo *trans*-TcO_2^+ cores are also of great importance in nuclear medicine,[16,17,19] and there have been recent indications that these species may also undergo in vivo redox reactions that affect their biodistributions.[22] However, only a few electrochemical investigations of oxo–technetium(V) complexes have been reported, primarily because these species do not generally undergo electrochemically reversible redox processes.[23,24] We have recently observed[25,26] that oxo–rhenium(V) complexes containing Schiff base ligands exhibit reversible electrochemical reactions and thus thought that a study of the analogous oxo–technetium(V) com-

---

(1) CNR.

(2) University of Cincinnati.

(3) Universitá di Sassari.

(4) Mazzocchin, G. A.; Seeber, R.; Mazzi, U.; Roncari, E. *Inorg. Chim. Acta* **1977**, *29*, 5.

(5) Mazzi, U.; Roncari, E.; Seeber, R.; Mazzocchin, G. A. *Inorg. Chim. Acta* **1980**, *41*, 95.

(6) Seeber, R.; Mazzocchin, G. A.; Roncari, E.; Mazzi, U. *Transition Met. Chem.* (*London*) **1981**, *6*, 123.

(7) Hurst, R. W.; Heineman, W. R.; Deutsch, E. *Inorg. Chem.* **1981**, *20*, 3298.

(8) Roncari, E.; Mazzi, U.; Seeber, R.; Zanello, P. *J. Electroanal. Chem. Interfacial Electrochem.* **1982**, *132*, 221.

(9) Seeber, R.; Mazzocchin, G. A.; Mazzi, U.; Roncari, E.; Refosco, F. *Transition Met. Chem.* (*London*) **1984**, *9*, 315.

(10) Ichimura, A.; Heineman, W. R.; Vanderheyden, J.-L.; Deutsch, E. *Inorg. Chem.* **1984**, *23*, 1272.

(11) Bandoli, G.; Mazzi, U.; Ichimura, A.; Libson, K.; Heineman, W. R.; Deutsch, E. *Inorg. Chem.* **1984**, *23*, 2898.

(12) Jurisson, S. S.; Dancey, K.; McPartlin, M.; Tasker, P. A.; Deutsch, E. *Inorg. Chem.* **1984**, *23*, 4743.

(13) Ichimura, A.; Heineman, W. R.; Deutsch, E. *Inorg. Chem.* **1985**, *24*, 2134.

(14) Kirchhoff, J. R.; Heineman, W. R.; Deutsch, E. *Inorg. Chem.* **1987**, *26*, 3108.

(15) Vanderheyden, J.-L.; Heeg, M. J.; Deutsch, E. *Inorg. Chem.* **1985**, *24*, 1666.

(16) Deutsch, E.; Libson, K.; Jurisson, S.; Lindoy, L. F. *Prog. Inorg. Chem.* **1983**, *30*, 75.

(17) Deutsch, E.; Libson, K. *Comments Inorg. Chem.* **1984**, *3*, 83.

(18) Deutsch, E.; Libson K.; Vanderheyden, J.-L.; Ketring, A. R.; Maxon, H. R. *Nucl. Med. Biol.* **1986**, *13*, 465.

(19) Clarke, M. J.; Podbielski, L. *Coord. Chem. Rev.* **1987**, *78*, 253.

(20) Doyle, M. N.; Libson, K.; Woods, M.; Sullivan, J. C.; Deutsch, E. *Inorg. Chem.* **1986**, *25*, 3367.

(21) Libson, K.; Doyle, M. N.; Thomas, R. W.; Nelesnik, T.; Woods, M.; Sullivan, J. C.; Elder, R. C.; Deutsch, E. *Inorg. Chem.* **1988**, *27*, 3614.

(22) Neirinckx, R. D.; Harrison, R. C.; Forster, A. M.; Burke, J. F.; Anderson, A. R.; Lassen, N. A. *J. Nucl. Med.* **1987**, *28*, 559.

(23) Jurisson, S.; Lindoy, L. F.; Dancey, K. P.; McPartlin, M.; Tasker, P. A.; Uppal, D. K.; Deutsch, E. *Inorg. Chem.* **1984**, *23*, 227.

(24) Vanderheyden, J.-L; Ketring, A. R.; Libson, K.; Heeg, M. J.; Roecker, L.; Motz, P.; Whittle, L. R.; Elder, R. C.; Deutsch, E. *Inorg. Chem.* **1984**, *23*, 3184.

(25) Seeber, R.; Mazzocchin, G. A.; Mazzi, U.; Refosco, F.; Tisato, F. *Polyhedron* **1986**, *5*, 1975.

(26) Seeber, R.; Mazzocchin, G. A.; Refosco, F.; Mazzi, U.; Tisato, F. *Polyhedron* **1987**, *6*, 1647.

0020-1669/88/1327-4121$01.50/0